Aluminium(III)–Pyrocatechol Violet Equilibria: a Potentiometric Study

Stuart L. Simpson,[a] Staffan Sjöberg[b] and Kipton J. Powell[a]

[a] *Department of Chemistry, University of Canterbury, Private Bag 4800, Christchurch, New Zealand*

[b] *Department of Inorganic Chemistry, University of Umeå, S-901 87 Umeå, Sweden*

The equilibrium reactions between aluminium(III) and the dye pyrocatechol violet {2-[(3,4-dihydroxyphenyl)(3-hydroxy-4-oxocyclohexa-2,5-dien-1-ylidene)methyl]benzenesulfonic acid, H_4L} have been studied by potentiometric titration in aqueous solution, $I = 0.10$ mol dm^{-3} K(Cl), 25.0 °C. Equilibrium constants log β_{pqr} for the reactions $pH^+ + qAl^{3+} + rH_3L^- \rightleftharpoons H^+{}_pAl^{3+}{}_q(H_3L^-)_r^{p+3q-r}$ were determined, as were the dye deprotonation constants, log $\beta_{-n,0,1}$ ($n = 1$–3). The dye displayed both quinonoid and 1,2-dihydroxyaryl binding. The data were interpreted in terms of a series of complexes $[Al(H_2L)_n]^{(3-2n)+}$ (quinonoid binding) forming at $-\log h < 4.5$, where h is the free hydrogen-ion concentration, whereas at high $-\log h$ values the 1,2-dihydroxyaryl complexes $[Al(HL)_nL_{3-n}]^{(n-9)+}$ ($n = 1$–3) form. Mixed-site binding occurred at intermediate $-\log h$ values. Calculations confirmed that $-\log h = 5.6$–6.5 is optimum for spectrophotometric measurements, with a 1:2 complex dominating in this range. Modelling calculations indicated that the presence of gibbsite colloids in natural waters could lead to a significant error in the determination of Al^{3+}.

Aluminium is toxic towards many plants and environmental organisms.[1] In humans, dementia disorders have been related to elevated levels and accumulation of aluminium.[2] Elevated levels of aluminium in soils and freshwaters, from acidification, have been correlated with reduced crop yields[3,4] and reduction of fish populations.[5]

A range of metallochromic dyes have been used for spectrophotometric or fluorescence immunassay spectrophotometric analysis of aluminium in environmental systems, *e.g.* pyrocatechol violet,[6,7] chrome azurol S,[8] eriochrome cyanine R,[6] oxine[9] and aluminon.[6] Several comparisons have been made between selected ligands.[6,8,9]

The most common methods for measuring the toxic aluminium species are fractionation techniques using the Barnes–Driscoll protocol.[10–12] These involve separation of inorganic monomeric (labile) Al from organic monomeric (non-labile) Al on a cation-exchange column, followed by determination of the total, labile and non-labile, Al. Pyrocatechol violet is commonly used for analysis of Al in each fraction. In general these procedures are operationally defined,[13] making direct comparison of results from different techniques difficult because of poorly quantified kinetic and thermodynamic factors.

Several spectrophotometric studies of equilibria between aluminium and pyrocatechol violet {2-[(3,4-dihydroxyphenyl)(3-hydroxy-4-oxocyclohexa-2,5-dien-1-ylidene)methyl]-benzenesulfonic acid, H_4L} have been reported.[14,15] However, none of these has adequately analysed the equilibria. In a potentiometric study the formation of three complexes was proposed and equilibrium constants were given,[16] however the values are anomalously high for 'catecholate' ligands. The lack of reliable data for H^+–Al^{3+}–H_4L equilibria contributes to confusion over which aluminum species are being targeted during spectrophotometric analyses, *e.g.* in the 60 s measurements of reactive Al in soil solutions.[17]

This paper reports the equilibrium constants for the H^+–Al^{3+}–H_4L system in 0.1 mol dm^{-3} K(Cl) medium at 25.0 °C, *viz.* log β_{pqr} for $pH^+ + qAl^{3+} + rH_3L^- \rightleftharpoons H^+{}_pAl^{3+}{}_q(H_3L^-)_r^{p+3q-r}$.

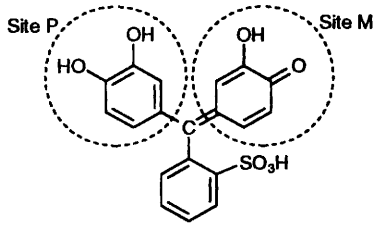

H_4L

Experimental

Chemicals and Analysis.—Reagent grade pyrocatechol violet (Koch-Light, Merck) was dried to constant weight at 110 °C under vacuum to remove occluded acidic impurities prior to solution preparation. Attempts at recrystallization were unsuccessful. Solutions of it were membrane filtered (−0.025 μm). However, small amounts of foreign acidic substances remained. The dye and 'dirt acid' concentrations in stock solutions were determined from potentiometric titration data using the computer program LAKE.[18] The dye content was found to be within 1–2% of the value expected from weighing; the remaining weight was assumed to be that of occluded water or 'dirt acid'. A stock solution of Al^{3+} (*ca.* 0.1 mol dm^{-3}) was prepared from $AlCl_3 \cdot 6H_2O$ (Baker Analysed Reagent) in *ca.* 0.1 mol dm^{-3} HCl and standardized by back titration of an excess of ethylenediamine-*N*,*N*,*N*′,*N*′-tetraacetate (edta) with $Pb(NO_3)_2$ using xylenol orange indicator. The content of Al^{3+} determined was within 0.1% of the weighed amount. The content of H^+ in this solution was standardized coulometrically. Carbonate-free potassium hydroxide solutions were prepared from a saturated (*ca.* 16 mol dm^{-3}) KOH (Eka Nobel, *p.a.*) solution. Dilute (*ca.* 0.01–0.04 mol dm^{-3}) KOH solutions were standardized potentiometrically against standard HCl. Hydrochloric acid solutions (Merck, *p.a.*) were standardized against tris(hydroxymethyl)methylamine (Trizma-base, Sigma) or coulometrically. All solutions were prepared from CO_2-free,

boiled Milli-Q water and all working solutions were prepared in 0.100 mol dm^{-3} K(Cl) (Merck, *p.a.*), dried at 120 °C.

Apparatus.—The automatic system for precise electromotive force (e.m.f) titrations, the thermostat and the electrodes and calibration procedures were described previously.[19] Stirring was effected with a Teflon magnetic stirrer bar. Under titration, the solution was protected from the intrusion of atmospheric oxygen and carbon dioxide by passing a continuous flow of argon over it. The gas was first bubbled through solutions of 10% KOH and 10% H_2SO_4 to remove acid and alkaline impurities and then through a solution of pyrogallate (benzene-1,2,3-triolate) in 1 mol dm^{-3} KOH. Finally, before the gas came into contact with the equilibrium solution it was passed through pure ionic medium solution (0.1 mol dm^{-3} KCl).

The free hydrogen-ion concentration, h, was determined by measuring the e.m.f of the cell Ag,AgCl(s) | 0.100 mol dm^{-3} KCl || equilibrium solution | glass electrode. Assuming the activity coefficients to be constant, the expression (1) is valid for the

$$E = E_0 + 59.157 \cdot \log h + E_j \quad (1)$$

measured e.m.f, where E_0 is a constant determined prior to each titration in a series of solutions of known hydrogen-ion concentration at $-\log h < 3.8$. (This was carried out *via* coulometric reductions of H^+ in a dilute HCl solution.) The liquid-junction potential, E_j, was calculated from E_j (mV) = $j_{ac}h + j_{alk}k_W h^{-1}$, where $\log k_W = -13.775$ is the ionic product of water and $j_{ac} = -511.5$ and $j_{alk} = 238.7$ mV dm^3 mol^{-1} are liquid-junction parameters in 0.100 mol dm^{-3} medium.[20] In the present investigation j_{ac} was determined as $-519 \pm 34(3\sigma)$ mV dm^3 mol^{-1} which is in good agreement with the value above (used in the calculations).

Visible absorption spectra were recorded on a Perkin-Elmer Lambda 2 UV/VIS spectrophotometer. A peristaltic pump was used to circulate solution through a 10 mm flow cell (70 μl) in the spectrophotometer.

Titrations.—Titrations for determination of the dissociation constants $\log \beta_{-1,0,1}$ and $\log \beta_{-2,0,1}$ for the dye and $\log k_D$ for the 'dirt acid' were performed separately within the ranges $0.002 \leqslant C \leqslant 0.01$ mol dm^{-3} and $2.0 \leqslant -\log h \leqslant 9.5$ (where C = total concentration of dye). Coulometric titrations of the dye were prevented by an indeterminate side reaction. This phenomenon has been reported previously for pyrocatechol.[21]

In three-component titrations B and C were varied within the limits $0.0004 \leqslant B \leqslant 0.006$ and $0.002 \leqslant C \leqslant 0.010$ mol dm^{-3}, covering C/B in the range 1–10 (B denotes the total aluminium concentration). Dilution titrations were performed at $C/B = 1$ by addition of aliquots of Al–H_4L solution (prepared *via* titration to $3.5 \leqslant -\log h \leqslant 4.0$) to pure ionic medium.

The reproducibility and reversibility of equilibria were tested by performing both forward (increasing $-\log h$) and backward (decreasing $-\log h$) titrations.

Spectrophotometric Determination of log $\beta_{-3,0,1}$.—This determination required rigorous exclusion of oxygen. The thermostatted cell (total volume *ca.* 120 cm^3) was sealed by ground-glass flanges. One port in the lid accommodated a Gilmont micrometer syringe passing through a bored rubber stopper; a second port contained a ground-glass stopper with attached plastic strings suspending a small glass boat containing Analar KOH pellets. Two small central ports accommodated a nitrogen gas line and microline tubing which connected the titration cell to a spectrophotometric cell (70 μl) *via* a peristaltic pump. Nitrogen gas was deoxygenated first *via* an acidic vanadium(II) solution over a zinc (mercury) amalgam, followed by pyrogallate in 1 mol dm^{-3} KOH solution. Oxygen-free nitrogen was passed over the dye solution, both during the spectrophotometric measurements and for 2 h before.

Data Treatment

Potentiometry.—Data treatment assumed the presence of three-component equilibria of the general form (2a) and the two-component equilibria (2b) and (2c). The law of mass action

$$\beta_{pqr}: \quad pH^+ + qAl^{3+} + rH_3L^- \rightleftharpoons H_pAl_q(H_3L)_r^{(p+3q-r)+} \quad (2a)$$

$$\beta_{pq0}: \quad pH^+ + qAl^{3+} \rightleftharpoons H_pAl_q^{(p+3q)+} \quad (2b)$$

$$\beta_{p01}: \quad pH^+ + H_3L^- \rightleftharpoons H_{3+p}L^{(p-1)+} \quad (2c)$$

and the conditions for the total concentrations then give equations (3)–(5), where $b = [Al^{3+}]$ and $c = [H_3L^-]$. The

$$H = h + \Sigma p\beta_{p01}h^p c + \Sigma p\beta_{pq0}h^p b^q + \Sigma p\beta_{pqr}h^p b^q c^r - k_w h^{-1} \quad (3)$$

$$B = b + \Sigma q\beta_{pq0}h^p b^q + \Sigma q\beta_{pqr}h^p b^q c^r \quad (4)$$

$$C = c + \Sigma\beta_{p01}h^p c + \Sigma r\beta_{pqr}h^p b^q c^r \quad (5)$$

summations are taken over all species formed; β_{pqr}, β_{pq0} and β_{p01} are the equilibrium constants for the reactions (2a), (2b) and (2c), respectively.

The aluminium hydrolysis species, defined according to equation (2b), were: $[Al(OH)]^{2+}$ ($\log \beta_{-1,1,0} = -5.33$), $[Al(OH)_2]^{2+}$ ($\log \beta_{-2,1,0} = -10.91$), $[Al_3(OH)_4]^{5+}$ ($\log \beta_{-4,3,0} = -13.13$), $[Al_{13}(OH)_{32}]^{7+}$ ($\log \beta_{-32,13,0} = -107.41$) and $[Al(OH)_4]^-$ ($\log \beta_{-4,1,0} = -23.46$).[21,22]

Since the dissociation of the sulfonate proton occurs at $-\log h < 1$,[23] the zero level is defined as a triprotic species, H_3L^-. The least-squares computer program LAKE[18] was used to determine sets of *pqr* triplets and the corresponding equilibrium constants which 'best' fit the experimental data. The best model was the one which gave the lowest error squares sum $U_{ZC} = [(H_{calc} - H_{expt})/C]^2$. Goodness-of-fit parameters are expressed as $U_{ZC}(pr)_q \times 10^{-3}$ and $\sigma(Z_C)$ where *pqr* designate the species present [*i.e.* $U_{Z_c}(00)_0$ is U_{Z_c} before new species were included] and $Z_C(-\log h) = (h - H - k_w h^{-1})/C$.

Spectrophotometry.—The constant $\log \beta_{-3,0,1}$ was calculated by Ågren's method.[24] Ligand absorption spectra were determined for six wavelengths (in the range 460–550 nm) as a function of $-\log h$ (11.5–12.8). The molar absorption coefficient, ε, for the fully deprotonated species was determined following addition of KOH(s) to the cell.

Data, Calculations, Results

The experimental results showing the complexation behaviour of the system are illustrated by the function $Z_C(-\log h)$, *i.e.* the average number of OH^- reacted per dye molecule plotted as a function of $-\log h$ (Fig. 1).

The data used to calculate $\log \beta_{-1,0,1}$ and $\log \beta_{-2,0,1}$ and $\log k_D$ for the 'dirt acid' comprised 15 titrations with *ca.* 600 data points. The calculations established $\log \beta_{-1,0,1}$ ($\pm 3\sigma$) = -7.71 ± 0.01, $\log \beta_{-2,0,1} = -17.49 \pm 0.02$ and $\log k_D = -4.1 \pm 0.3$. The first protonation constant was calculated spectrophotometrically as $\log K_1 = 12.72 \pm 0.03$, giving $\log \beta_{-3,0,1} = -30.21 \pm 0.05$. The concentrations of 'dirt acid' and values of $\log k_D$ differed slightly between dye stock solutions. No solution was used for studying the H^+–Al^{3+}–H_4L system if the difference between the weighed and determined concentration of dye was greater than 2%.

Prior to numerical analysis of the three-component system, a simulation of the expected complexation properties of pyrocatechol violet was made by using the substances catechol[21] and maltol (3-hydroxy-2-methyl-4*H*-pyran-4-one)[25] in equal and representative concentrations. Here catechol is taken to approximate the 1,2-dihydroxyaryl binding site and maltol the 2-hydroxy-1-oxocyclohexadiene (quinonoid) site.

From the calculations it was seen that the 'maltol' site would be expected to dominate aluminium binding at lower $-\log h$ values, whereas the 'catechol' site would not be expected to bind a significant fraction of aluminium until $-\log h > 7$.

The analysis of the three-component data, comprising 27 titrations with 780 data points, was broken into two parts. The first comprised data with $C/B \geqslant 4$ selected to avoid any effects from possible polymeric hydroxo species that might exist at lower ratios. Initial calculations indicated that the formation of polynuclear species would be negligible under these conditions. The model calculation described indicated that a series of mononuclear maltol complexes, $[Al(H_2L)]^+$, $[Al(H_2L)_2]^-$ and $[Al(H_2L)_3]^{3-}$, could be expected to form at lower $-\log h$ values. The formation constants for these three species were evaluated from data for 10 titrations (182 data points with $2.2 \leqslant -\log h \leqslant 4.0$) by use of the program LAKE.

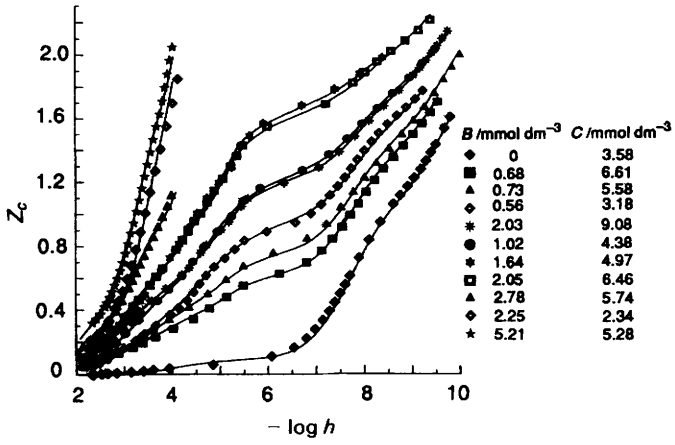

Fig. 1 Part of the experimental data plotted as curves $Z_C(-\log h) = (h - H - k_w h^{-1})/C$ for C/B ratios 1, 2, 3, 4.5, 5.7, 7.5, 10 and ∞. The Z_C function was calculated over the zero-proton level H_2O, Al^{3+}, H_3L^-. All symbols represent total concentrations of Al and dye. The curves were calculated using the constants in Table 1

The equilibrium constants obtained were $\log \beta_{-1,1,1} = -0.19 \pm 0.05$, $\log \beta_{-2,1,2} = -1.05 \pm 0.05$ and $\log \beta_{-3,1,3} = -2.53 \pm 0.09$.

These three species were then considered as known and a complete *pqr* analysis (the testing of single triplets or combinations of triplets) was performed on 10 titrations (175 data points, $3.7 \leqslant -\log h \leqslant 7.0$) to find species which best explained the experimental data up to $-\log h = 7.0$. These calculations, for which U_{ZC} values are given in Fig. 2(*a*), indicated four compositions that could equally well explain most of the experimental data. However, a comparison of experimental with theoretical Z_C curves revealed systematic residuals still remaining, thereby indicating a need for at least one further species to be included in the model. A second *pqr* analysis was therefore undertaken which successively included one of the four 'best' species indicated in Fig. 2(*a*) in combination with a second species with another *pqr* composition. The results of these calculations indicated significant improvement in U_{ZC} for only two of the four 'best' species. These results are presented in Fig. 2(*b*) and 2(*c*). For the other two 'best' species no improvement was obtained by including a second species. Fig. 2 shows that the combination of the species (−4,1,2) ($\log \beta_{-4,1,2} = -10.26 \pm 0.10$) and (−5, 1,3) ($\log \beta_{-5,1,3} = -13.03 \pm 0.13$) gives the best fit to the experimental data, $U_{Z_c}(pr)_q \times 10^{-3} = 0.72$ and $\sigma(Z_C) = 0.004$.

For the remaining data, to $-\log h = 9.6$, the logical species remaining that could be included in the model were (−6,1,3), *i.e.* $[Al(HL)_3]^{6-}$, followed by the stepwise deprotonated species (−7,1,3) $[Al(HL)_2L]^{7-}$, (−8,1,3) $[Al(HL)L_2]^{8-}$ and (−9,1,3) $[AlL_3]^{9-}$. Statistical approximations[26] were used to provide initial estimates of the equilibrium constants for the last two species. Calculations indicated that there would be no measurable concentration of $[AlL_3]^{9-}$ below $-\log h = 9.6$ and this species was not included in further analysis. Use of this series of complexes adequately explained all remaining data. In a final calculation on this data set (10 titrations and 447 data points, $2.2 \leqslant -\log h \leqslant 9.6$) the equilibrium constants for all the above species except (−9,1,3) were varied on the whole data set.

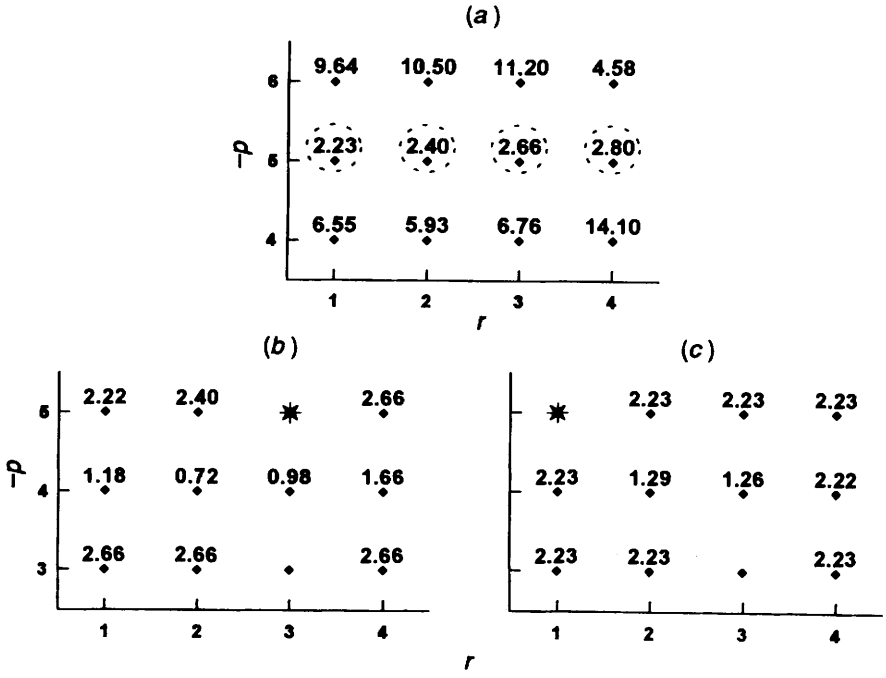

Fig. 2 Results of the *pqr* analysis ($q = 1$) concerning the range $3.7 \leqslant -\log h \leqslant 7.0$. The diagrams give the error squares sums $U_{Z_c}(pr)_q \times 10^{-3}$, assuming one new complex in (*a*) and two in (*b*) and (*c*) respectively. The four 'best' species are circled in (*a*). In (*b*) and (*c*) the complex assumed known, from (*a*), has been starred and the $U_{Z_c}(pr)_q$ value given is the error-squares sum for the combination of this species, also refined, with another *pqr* species, as shown. In the calculations, equilibrium constants for aluminium hydrolysis and the species $[Al(H_2L)]^+$, $[Al(H_2L)_2]^-$ and $[Al(H_2L)_3]^{3-}$ have been assumed to be known, *cf.* the absence of error-squares sum at (−3,1,3). The calculations were based on 175 points giving an initial sum of squares $U_{Z_c}(00)_0 \times 10^{-3} = 60.9$

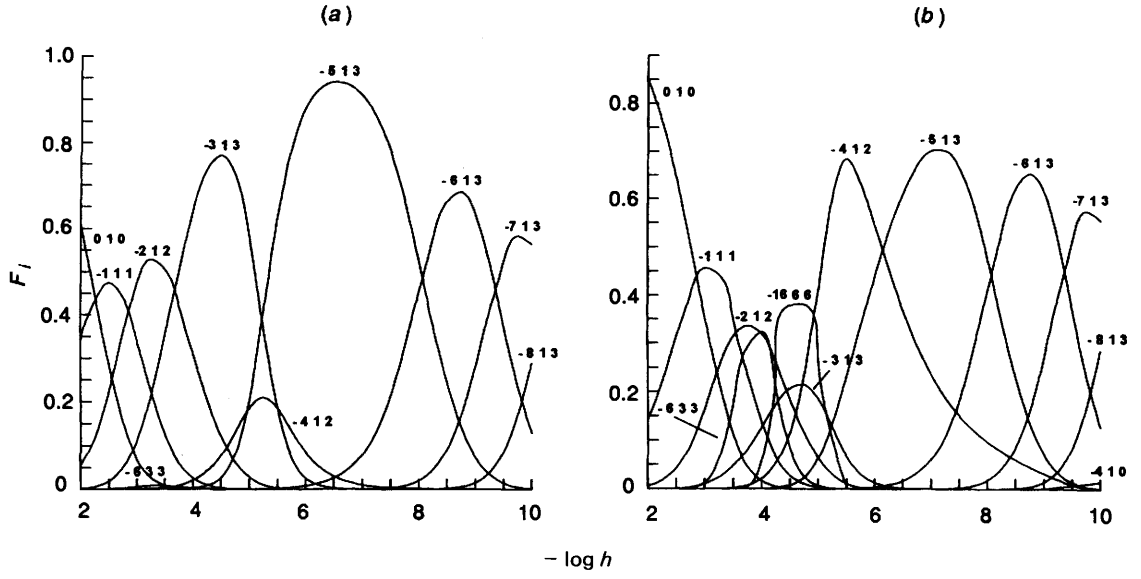

Fig. 3 Distribution diagrams $F_i(-\log h)_{B,C}$ for millimolar concentrations of the dye and Al^{3+}; F_i is defined as the ratio of the aluminium concentration in an equilibrium species to the total aluminium concentration. The calculations have been performed with the computer program SOLGASWATER with the equilibrium constants given in Table 1. B = 1.0 mmol dm^{-3}, C = 10.0 (*a*) or 3.0 mmol dm^{-3} (*b*)

Table 1 Binary and ternary complexes in the H^+–Al^{3+}–pyrocatechol violet system. The equilibrium constants (β_{pqr}) are given according to the reaction $pH^+ + qAl^{3+} + rH_3L^- \rightleftharpoons H_pAl_q(H_3L)_r^{p+3q-}$

p,q,r	log (β_{pqr} ± 3σ)	Proposed formula
−1,0,1	−7.71 ± 0.01	H_2L^{2-}
−2,0,1	−17.49 ± 0.02	HL^{3-}
−3,0,1	−30.21 ± 0.05	L^{4-}
−1,1,1	−0.23 ± 0.04	$[Al(H_2L)]^+$
−2,1,2	−1.02 ± 0.03	$[Al(H_2L)_2]^-$
−3,1,3	−2.57 ± 0.06	$[Al(H_2L)_3]^{3-}$
−4,1,2	−10.21 ± 0.09	$[Al(HL)_2]^{3-}$
−5,1,3	−13.03 ± 0.11	$[Al(H_2L)(HL)_2]^{5-}$
−6,1,3	−21.10 ± 0.14	$[Al(HL)_3]^{6-}$
−7,1,3	−30.46 ± 0.25	$[Al(HL)_2L]^{7-}$
−8,1,3	−40.75 ± 0.46	$[Al(HL)L_2]^{8-}$
−9,1,3	−52.0 (estimate)	$[AlL_3]^{9-}$
−6,3,3	−5.07 ± 0.05	$[Al_3(H_2L)_3(OH)_3]$
−16,6,6	−23.2 ± 0.2	$[Al_6(H_2L)_6(OH)_{10}]^{4-}$

Table 2 Deprotonation and stability constants for catechol[a] and maltol[b]

Compound	p,q,r	log (β_{pqr})	Formula
Catechol (H_2L)	−1,0,1	−9.26	HL^-
	−2,0,1	−22.69	L^{2-}
	−2,1,1	−5.80	$[AlL]^+$
	−4,1,2	−14.83	$[AlL_2]^-$
	−6,1,3	−28.54	$[AlL_3]^{3-}$
Maltol (HL)	−1,0,1	−8.38	L^-
	−1,1,1	−0.13	$[AlL]^{2+}$
	−2,1,2	−0.96	$[AlL_2]^+$
	−3,1,3	−2.67	$[AlL_3]$

[a] 0.1 mol dm^{-3} KCl.[30] [b] 0.6 mol dm^{-3} NaCl.[25]

The second part of these calculations involved the analysis of data at C/B < 3.5. These calculations involved the use of 14 titrations, including three dilution titrations, and 280 data points over the range $2.2 \leqslant -\log h \leqslant 4.2$. An initial comparison of experimental and theoretical curves indicated almost no remaining Z_C residuals for 3.0 < C/B < 3.5, however very large deviations could be seen at C/B < 2.1. Once again *pqr* analyses were performed on the experimental data to obtain the sets of *pqr* triplets giving the lowest value of U_{ZC} and thus best explaining the data. Preliminary analyses indicated that simple mononuclear species had little effect on improving the fit. Results from *pqr* analyses with q = 1, 2, 3, 4 or 5 showed that the species which could 'best' explain the data were those with r/q = 1 and $2 \leqslant q \leqslant 4$. However, no single species was adequate to explain all the data; therefore combinations of two species with r/q = 1 were considered. These calculations indicated that the combination of a species with $r = q = 3$ and another with r/q = 1 was adequate. The final result from these calculations was the inclusion of one species with $r = q = 3$ (log $\beta_{-6,3,3} = -5.07 \pm 0.05$) and another with $r = q = 6$ (log $\beta_{-16,6,6} = -23.2 \pm 0.2$). This gave $U_{ZC}(pr)_q \times 10^{-3} = 6.6$ and $\sigma(Z_C) = 0.02$, where $U_{ZC}(00)_0 \times 10^{-3} = 415.4$. The effect of these two species on the equilibrium constants determined for data with C/B > 4 was checked *via* a calculation using both data sets over the range $2.2 \leqslant -\log h \leqslant 9.6$. The result indicated that the polynuclear species described above had very little effect on the species forming at higher values of C/B. The final results for all species forming in the binary and ternary systems are given in Table 1 and the fit of experimental data by the resulting theoretical curves is seen in Fig. 1.

With this final model, no systematic deviations remained. The computer program SOLGASWATER[27] was used to calculate distribution diagrams. These are presented in Fig. 3.

Discussion

The dye deprotonation constants log $\beta_{-n,0,1}$ in Table 1 are in reasonable agreement with those reported by other workers at the same ionic strength (−7.77, −17.52[28] and −7.90, −17.84;[29] n = 1,2). However, the values determined previously for the third deprotonation constant (−11.71 and −11.82, n = 3, respectively) are significantly lower than that reported here [log ($\beta_{-3,0,1}/\beta_{-2,0,1}$) = −12.72]. This difference may be related to the propensity of the dye to undergo oxidation at high −log h values and the resulting difficulty in accurately determining this dissociation constant. In our study log K_1 was determined under strictly oxygen-free conditions. This value can be compared with that for catechol [log ($\beta_{-2,0,1}/\beta_{-1,0,1}$) −13.43, Table 2].

The order in which the OH groups deprotonate may be

deduced from the spectral shifts occurring with changes in $-\log h$ and from the structure of the dye molecule. The large colour change from orange-red (λ_{max} = 442 nm) to blue-violet (λ_{max} = 585 nm) that accompanies the first deprotonation indicates that proton loss is from the 1,2-dihydroxyaryl moiety, probably the *para*-OH. Deprotonation of the hydroxy group on the quinonoid moiety would not be expected to develop enough electron delocalization for such a colour change. This assignment of protonation constant indicates that in pyrocatechol violet the 1,2-dihydroxyaryl moiety has a significantly higher acidity than does catechol (−9.26, Table 2). This can be rationalized in terms of the electron-withdrawing properties of the quinonoid moiety. A direct comparison of the acidity of the latter with model compounds is not possible but it is noted that the OH group is significantly less acidic than the OH in maltol (Table 2).

Regarding the three-component system, the species in this series, $[Al(H_2L)_n]$ (n = 1–3), which form at $-\log h < 4.5$ are probably chelates between Al^{3+} and the quinonoid moiety (site M). At higher $-\log h$ values the species forming more likely involve the 1,2-dihydroxyaryl moiety (site P) of the dye. These deductions are based on the simulation of its expected complexation properties. Catechol is an appropriate model for the 1,2-dihydroxyaryl moiety, and maltol should approximate to the binding properties of the quinonoid moiety. The inductive effects for maltol will be significantly different due to the pyranone oxygen. At intermediate $-\log h$ values there is the possibility of mixed-site binding. This is consistent with the species composition (−5,1,3), *i.e.* $[Al(H_2L)(HL)_2]^{5-}$.

A comparison may be made between the present results (Table 1) and the aluminium equilibria for catechol and maltol (Table 2). Similarities are apparent between the constants obtained for the species (−1,1,1), (−2,1,2) and (−3,1,3) of maltol, AlL_n, and the dye, $Al(H_2L)_n$. However significant differences are noted for the species (−4,1,2) and (−6,1,3) of catechol, AlL_2, AlL_3 in comparison to the dye, $Al(HL)_2$, $Al(HL)_3$. In the Al^{3+}–dye system the equivalent species form at a lower $-\log h$ than in the Al^{3+}–catechol system. This can be explained by the much larger first (and larger second) deprotonation constant for the 1,2-dihydroxyaryl moiety in the dye compared to that of catechol. Modelling calculations indicated that the 'catechol' site would not bind a significant fraction of aluminium until $-\log h > 7$. Owing to the stronger binding by the 1,2-dihydroxyaryl moiety in the dye, this site begins to dominate aluminium binding at *ca.* $-\log h = 5$, *i.e.* lower than predicted from the modelling and consistent with the higher acidity of this moiety. The only other stability constants for the H^+–Al^{3+}–dye system were determined by Goina *et al.*[16] Their results (log K_n = 25.12, 22.27 and 20.74, n = 1–3 respectively) are anomalously high compared with other catecholate ligands.

The observation that a series of one-proton reactions occurs at $-\log h > 8$ is consistent with (*i*) complexes having the 1,2-dihydroxyaryl moiety binding to Al {as in $[Al(HL)_3]^{6-}$, $[Al(HL)_2L]^{7-}$, *etc.*}, and (*ii*) the assignment of the second protonation constant of the free dye to the OH group on the quinonoid moiety. The pK_a calculated for formation of $[Al(HL)L_2]^{8-}$ from $[Al(HL)_2L]^{7-}$ (10.29) is significantly higher than that of the group presumed to be deprotonating (9.78 for the free dye); it is also higher than estimated from statistical considerations (9.36 + log 3) where $\log \beta_{-7,1,3} - \log \beta_{-6,1,3} = 9.36$. This observation may indicate that disturbance of the charge distribution by the aluminium centre significantly affects the dissociation of the conjugated pendant OH group; an apparent shift of > 0.4 occurs in the pK_a of the unco-ordinated quinonoid proton. Further, conjugation within the ligands means that the pendant quinonoid groups are not electronically independent. Dissociation of one such group {to form $[Al(HL)_2L]^{8-}$} affects the net phenoxide electron density about the Al^{3+} centre and lowers the acidity of the remaining pendant groups. A similar phenomenon has been reported previously for protocatechuic acid complexes of Al[30] where the apparent pK_a of the carboxy group was shifted by $\approx +0.4$. This contrasts with ligand systems where the co-ordinated and pendant groups are not conjugated; for example in the dopamine [4-(2-aminoethyl)benzene-1,2-diol] complexes of Al the dissociation constants for the non-co-ordinated NH_3^+ groups are statistically related.

Deprotonated pyrocatechol violet (H_2L^{2-}) can be represented by resonance structures involving conjugation between the quinonoid (M) site and the monoprotonated 1,2-dihydroxyaryl site (P). This conjugation provides a mechanism for Al^{3+} bound at site M to become bound by site P without altering its chelation position. The complex merely undergoes a deprotonation and an intramolecular electron shift. The formation of $[Al(HL)_2]^{3-}$ from the three-co-ordinated $[Al(H_2L)_3]^{3-}$ species can be thought of as arising from such a mechanism. The transition from a tris species $[Al(H_2L)_3]^{3-}$ to a bis species $[Al(HL)_2]^{3-}$ with increasing $-\log h$ may be rationalized in terms of the change in electron density surrounding the Al^{3+} centre. The charge stabilization effected by two deprotonated 1,2-dihydroxyaryl moieties should be at least equivalent to three deprotonated quinonoid moieties, resulting in a species of similar or greater stability.

Titrations at lower C/B ratios indicated the species (−6,3,3) $[Al_3(H_2L)_3(OH)_3]$ and (−16,6,6) $[Al_6(H_2L)_6(OH)_{10}]^{4-}$ are formed at $-\log h < 4.2$ (Fig. 3). These titrations were terminated at $-\log h < 4.2$ due to precipitation (observed in solutions with C/B = 1); this may be due to formation of polymerized or uncharged species. Calculations using the final constants indicated that these species exist up to $-\log h \approx 6.5$. It is possible that they represent the summation of a larger series of polynuclear hydroxo species. The verification of (−16,6,6) in the model required to fit the data at the higher $-\log h$ values was aided by dilution titrations. For these data polymers of low nuclearity were unable to explain the large systematic deviations recorded. The minimum in U_{ZC} was found at a nuclearity of six, whereby further increases in the nuclearity resulted in increased values of U_{ZC}. In studies of the related phthalein dye chrome azurol S (which has salicylate and 1-carboxy-2-oxocyclohexadiene residues), linear polymers (*e.g.* $Al_xH_{-x}L_{1+x}$, x = 4 or 5) were reported forming at $2.5 < -\log h < 6$.[31] The formation of such polymers is not possible for pyrocatechol violet because deprotonation and co-ordination of the 1,2-dihydroxyaryl moiety does not occur below $-\log h \approx 4$. Therefore these polymers must involve either hydroxy and/or *o*-quinonoid (O^-) bridges between adjacent Al^{3+} ions. Such polymeric units have been established for Al at low $-\log h$ in a great number of systems with organic ligands, *e.g.* in the citrate, $[Al_3(OH)(alkoxide)_3]$,[32] and lactate and propionate complexes, $[Al_2(OH)_2L]$.[33,34]

Spectrophotometric Analysis of Aluminium.—Determinations of Al in environmental samples are often carried out spectrophotometrically using the formation of an aluminium–pyrocatechol violet complex at $-\log h \approx 6$. From spectrophotometric molar ratio plots it has been found that the Al:dye ratio is 1:2 near pH 6 under spectrophotometric conditions ([dye] *ca.* 20 μmol dm^{-3}, $[Al^{III}]$ 0–10 μmol dm^{-3}). Calculations using SOLGASWATER were made with the constants from these studies (Table 1) to determine the species in solution at $-\log h = 6$ at spectrophotometric concentrations. The dominant species forming at $-\log h = 6$ was $[Al(HL)_2]^{3-}$ (Fig. 4), consistent with spectrophotometric molar ratio plots. This species dominates in the range $-\log h$ *ca.* 4.9–8.0. However its formation is (near) quantitative (> 95%) only in the range $-\log h$ = 5.6–6.5.

The suitability of a reagent for the analysis of Al will be impaired if it interacts with untargeted materials. Mineral oxides and clay materials are abundant in many natural waters and soil solutions. Much is within the colloidal range and would not be removed by a 0.45 μm filter. Therefore the potential

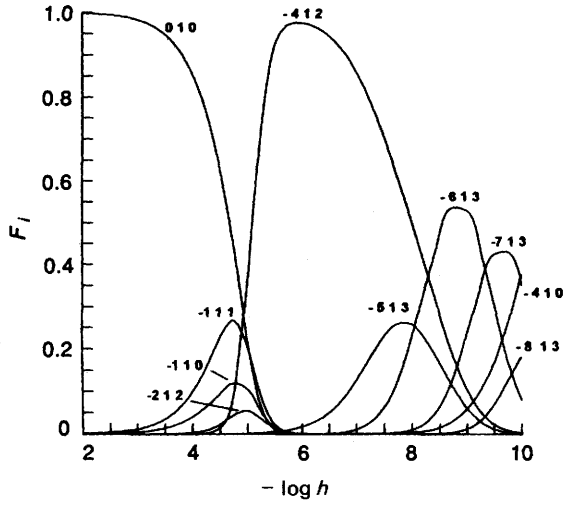

Fig. 4 Distribution diagrams $F_i(-\log h)_{B,C}$ for micromolar concentrations. Definition and method as for Fig. 3; $B = 0.004$, $C = 0.02$ mmol dm^{-3}

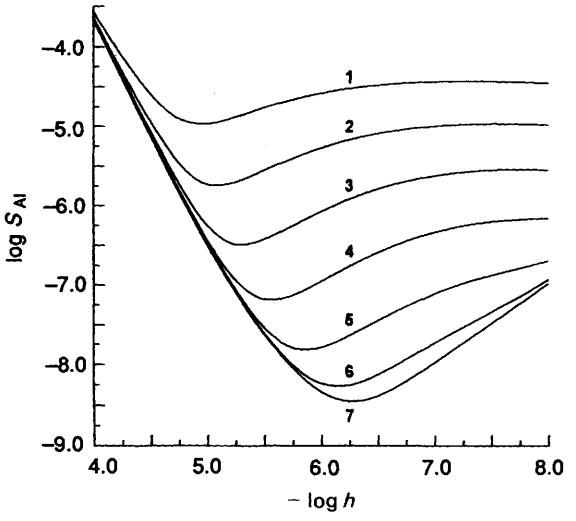

Fig. 5 The effects of pyrocatechol violet on the calculated solubility of gibbsite (log $*K_{s0} = 8.309$).[35] [dye] = 1×10^{-4} (1), $1 \times 10^{-4.5}$ (2), 1×10^{-5} (3), $1 \times 10^{-5.5}$ (4), 1×10^{-6} (5), $1 \times 10^{-6.5}$ (6) and 0 mol dm^{-3} (7)

solubilizing effects of pyrocatechol violet on natural mineral oxides was investigated by making a number of model calculations using the computer program SOLGASWATER. In these calculations a hypothetically 1 mol dm^{-3} solution of gibbsite (log $*K_{s0} = 8.309$)[35] was equilibrated with water and the dye. From Fig. 5 it can be seen that even at very low concentrations the dye increases the solubility of gibbsite over a large $-\log h$ range (if equilibrium is attained). At a typical analytical $-\log h$ (6.0) and dye concentration (30 μmol dm^{-3}) the effect of gibbsite (assuming equilibrium) would be to enhance the apparent concentration of Al in solution by *ca.* 5 μmol dm^{-3}. Attainment of equilibrium may require extremely long reaction times. It would, however, introduce a significant error in a typical working range of 0.5–10 μmol dm^{-3} Al. These calculations indicate that the error arising from the gibbsite dissolution will be minimized if (*i*) the dye is not used in large excess for spectrophotometric measurements, (*ii*) the $-\log h$ is kept as low as possible within the allowable window (5.8–6.6) for quantitative formation of $[Al(HL)_2]^{3-}$, and (*iii*) the reaction time is short to ensure the dissolution of gibbsite is minimal.

Acknowledgements

We thank Dr. Lars-Olof Öhman for constructive discussions throughout this work and comments on the manuscript. This work was financially supported by a University of Canterbury Doctoral Scholarship and the Swedish National Science Research Council.

References

1 B. O. Rosseland, T. D. Eldhuset and M. Staurnes, *Environ. Geochem. Health*, 1990, **12**, 17.
2 S. S. Krishnan, D. R. McLachlan, B. Krishnan, S. S. A. Fenton and J. E. Harrison, *Sci. Total Environ.*, 1988, **71**, 59.
3 A. D. Noble, M. E. Sumner and A. K. Alva, *Soil Sci. Soc. Am. J.*, 1988, **52**, 1059.
4 N. V. Hue, G. R. Craddrock and F. Adams, *Soil Sci. Soc. Am. J.*, 1986, **50**, 28.
5 J. P. Baker and C. L. Schofield, *Water, Air, Soil Pollut.*, 1982, **18**, 289.
6 O. Røyset, *Anal. Chim. Acta*, 1985, **178**, 223.
7 W. K. Dougan and A. L. Wilson, *Analyst (London)*, 1974, **99**, 413.
8 D. J. Hawke and H. K. J. Powell, *Anal. Chim. Acta*, 1994, **299**, 257.
9 S. C. Hodges, *Soil Sci. Soc. Am. J.*, 1987, **51**, 57.
10 R. B. Barnes, *Chem. Geol.*, 1975, **15**, 177.
11 C. T. Driscoll, *Int. J. Environ. Anal. Chem.*, 1984, **16**, 267.
12 B. Fairman, A. Sanz-Medel, M. Gallego, M.J. Quintela, P. Jones and R. Benson, *Anal. Chim. Acta*, 1994, **286**, 401.
13 J. Luster, A. Yang and G. Sposito, *J. Soil Sci. Soc. Am.*, 1993, **57**, 976.
14 V. N. Tikhonov and V. V. Bakhtina, *Zh. Anal. Khim.*, 1983, **39**, 2126.
15 E. Chiacchierini, D. Marini and A. Gagri, *Gazz. Chim. Ital.*, 1974, **104**, 1257.
16 T. Goina, M. Olariu and L. Bocaniciu, *IUPAC Stability Constants of Metal-Ion Complexes: Part B. Organic Ligands*, Pergamon, Oxford, 1979, p. 1130.
17 G. L. Kerven, D. G. Edwards, C. J. Asher, P. S. Hallman and S. Kokot, *Aust. J. Soil. Res.*, 1989, **27**, 91.
18 N. Ingri, A. Yagasaki, L. Andersson and K. Holmström, *Acta Chem. Scand.*, unpublished work.
19 L.-O. Öhman and S. Sjöberg, *Acta Chem. Scand., Ser. A*, 1981, **35**, 201.
20 S. Sjöberg, Y. Hägglund, A. Nordin and N. Ingri, *Mar. Chem.*, 1983, **13**, 35.
21 L.-O. Öhman and S. Sjöberg, *Polyhedron*, 1983, **2**, 1329.
22 P. L. Brown and R. N. Sylva, *J. Chem. Soc., Dalton Trans.*, 1985, 1967.
23 W. D. Wakley and L. P. Varga, *Anal. Chem.*, 1972, **44**, 169.
24 A. Ågren, *Acta Chem. Scand.*, 1955, **9**, 49.
25 T. Hedlund and L.-O. Öhman, *Acta Chem. Scand., Ser. A*, 1988, **42**, 702.
26 D. D. Perrin, B. Dempsey and E. P. Serjeant, *pK_a Prediction for Organic Acids and Bases*, Chapman and Hall, New York, 1981.
27 G. Eriksson, *Anal. Chim. Acta*, 1979, **112**, 375.
28 I. P. Saraswat, C. L. Sharma and A. Sharma, *J. Indian Chem. Soc.*, 1979, **56**, 928.
29 E. A. Biryuk and R. V. Ravitskaya, *Zh. Anal. Khim.*, 1970, **25**, 576.
30 J. A. Kennedy and H. K. J. Powell, *Aust. J. Chem.*, 1985, **38**, 659.
31 D. J. Hawke, S. Sjöberg and H. K. J. Powell, *Polyhedron*, 1995, **14**, 377.
32 L.-O. Öhman, *Inorg. Chem.*, 1988, **27**, 2565.
33 E. Marklund, Ph.D. Thesis, University of Umeå, 1990.
34 E. Marklund and L.-O. Öhman, *Acta Chem. Scand.*, 1990, **44**, 228.
35 D. A. Palmer and D. J. Wesolowski, *Geochim. Cosmochim. Acta*, 1992, **56**, 1093.

Received 28*th November* 1994; *Paper* 4/07224C